Vertical variations of Soil Carbon under Different Land Uses in a Karst Critical Zone Observatory (CZO), SW China

Caiqing Qin[a,b], Si-Liang Li[b*], Guang-Hui Yu[b], Adrian M. Bass[c], Fu-Jun Yue[b], Sheng Xu[b]

[a] Department of Earth & Environmental Science, School of Human Settlements and Civil Engineering, Xi'an Jiaotong University, Xi'an, 710049, China

[b] Institute of Surface-Earth System Science, School of Earth System Science, Tianjin University, Tianjin 300072, China

[c] School of Geographical and Earth Sciences, University of Glasgow, Glasgow G12 8QQ, United Kingdom

*Corresponding author:

Si-Liang Li (siliang.li@tju.edu.cn)

Fax: +86 22 27405053

Postal address: Institute of Surface-Earth System Science, Tianjin University, Tianjin 300072, China.

ABSTRACT

Soil is a key terrestrial carbon reservoir, a critical component of global carbon cycles, and in regulating climate change. Barren soils in karst zones have weak capacity for soil and water conservation and are readily erodible, making the carbon biogeochemical processes within karst soils potentially rapid and complex. To explore the vertical variation of soil carbon under karst conditions and its response to land-use change, this study investigated concentrations and isotopic compositions of both soil organic and inorganic carbon (SOC and SIC) in different depths of four land-use types in a typical karst region, SW China. Results show that as soil depth increases, SOC concentrations decrease, and its $\delta^{13}C$ ratios (from -27.3‰ to -19.4‰) increase in 0-20 cm depth but decrease at depths below 20 cm. The fresh SOC is mostly sequestered and cycled within the topsoil and subject to different controls than that of the subsoil. The turnover rate of SOC in karst soils does not directly co-vary with isotopic fractionation among different land uses. Long-term cultivation causes SOC loss from karst soils, which can be alleviated or even partially restored after farming cessation. SIC represents less than 10% of soil total carbon. The vertical heterogeneity of SIC variation and the direct influence of biological factors on SIC are both weaker relative to SOC. The low $\delta^{13}C$ ratios of SIC (from -20.4‰ to -3.0‰) indicate there is intense dissolution and reprecipitation of pedogenic carbonate within karst soil, especially in the upper cultivated layers. These results highlight that both SOC and SIC are labile and susceptible to land-use change in karst zones, which need to be considered in estimating karst carbon sink and its role in balancing global carbon budget on variable temporal scales.

Keywords: Soil organic carbon; Soil inorganic carbon; Carbon isotope; Vertical profiles; Land uses; Karst critical zone

1. Introduction

The terrestrial carbon (C) sink is an essential component for balancing the global C budget but gaps in our knowledge remain (Battin et al., 2009; Friedlingstein et al., 2020; Houghton, 2007). As the largest terrestrial C pool, soils store more C than the sum of living vegetation and the atmosphere (Falkowski et al., 2000; Schmidt et al., 2011). Soil C connects with both lateral C fluxes in water and vertical C fluxes via gaseous exchange, a minor alteration of which can potentially influence global C fate and subsequent climate change (Campeau et al., 2019; Davidson and Janssens, 2006; Stockmann et al., 2013). The soil C stock is also a reasonable proxy for soil fertility and productivity (Lehmann and Kleber, 2015; Mishra et al., 2021).

However, the estimations of both soil organic and inorganic C (SOC and SIC) stocks are still in debate, and can differ by orders of magnitude, at spatial scales ranging from regional to global (Batjes, 1996; Eswaran et al., 1995; Jobbágy and Jackson, 2000; Lal, 2004; Li et al., 2007; Mi et al., 2008; Wu et al., 2003). One major cause of uncertainty is the absence of detailed regional datasets of different soil types. As soils are asymmetrically distributed on Earth's surface, and soil C stock is also strongly interlinked to local climate, landforms, soil family level, land uses and rock outcrops (Bai and Zhou, 2020; Davidson and Janssens, 2006; Doetterl et al., 2015), soil C thus shows significant regional heterogeneity.

Interaction between SOC and SIC has been observed in several regions, and the specific mechanism and dominant controls likely respond to regional conditions and soil characteristics. In some regions, like Yanqi Basin and the Hebei Plain where soils are alkaline and have a higher SOC content than SIC, there was a positive correlation between SOC and SIC (Shi et al., 2017;

Wang et al., 2015). However, the contrary has also been measured in other studies (Hussain et al., 2019; Jelinski and Kucharik, 2009; Zhao et al., 2016). Soil pH, soil aggregation, hydrological processes and land uses were all regarded as driving factors (Deng et al., 2016; Zhang et al., 2020; Zhao et al., 2016) controlling this relationship. The regional interaction mechanism between SOC and SIC and corresponding dominant controls are thus potentially diverse and still not well elucidated and quantified. Therefore, local-scale investigations on soil C (both SOC and SIC) dynamics and stocks are critical for more accurately evaluating residual land C sinks and further constraining global C budgets.

Karst landforms cover 10-15% and ~35.9% of global and Chinese terrestrial surface area respectively (Ford and Williams, 2007; Yuan and Zhang, 2008). The C sink in karst regions is recognised, but likely underestimated (Pu et al., 2015; Zeng et al., 2019). Karst critical zones differ from non-karst systems in geomorphology, hydrogeology and soil development (Pain et al., 2020; Yuan and Zhang, 2008). Karst soils are usually thin, uneven, and vulnerable to erosion and desertification (Liu et al., 2009; Wang et al., 2004). These properties raise the possibility of significant C losses, eventually impairing soil fertility, hindering agricultural production further, and also increasing the difficulty to accurately evaluating SOC and SIC stocks in karst soils.

Carbon isotopic compositions have been confirmed as powerful proxies for tracing C sources and processes in terms of its distinct isotopic imprint among different sources and significant isotopic fractionations during various biogeochemical processes (Clark and Fritz, 1997). To our knowledge, studies on the coupled SOC and SIC dynamics in karst soils are still scarce using isotope techniques, especially on SIC which was reported to have a smaller global storage and a longer turnover time compared with SOC (Ding et al., 2016; Lal, 2004). However, karst characteristics, such as the thin soil layer, high hydrological connectivity (Zhang et al., 2021), the influence of carbonate weathering on soil formation (Moore et al., 2017), and the sensitivity of soil fertility to land use characteristics (Li et al., 2017), may significantly affect SIC processes and its interaction with SOC.

Thus, the Chenqi catchment, one typical karst critical zone observatory (CZO) located in Guizhou province, SW China, was selected as the research area to analyze soil C concentrations and isotopes in different land-use profiles. This study aimed to (1) explore the vertical variations of SOC and SIC within karst soils, and (2) assess the effects of land uses on karst soil C dynamics. We believe this to be the first systematic study to explore coupled SOC and SIC behaviors utilizing isotopes in different land-use soil profiles in a highly variable karst critical zone (K-CZ), which could provide useful insights into the research on karst soil C and supplement fundamental data sets for refining terrestrial C modeling.

2. Materials and methods

2.1. Research region and sampling sites

Chenqi catchment (26°15′20″-26°16′9″N, 105°46′3″-105°46′50″E, 1.25 km^2) is a CZO that reflects typical characteristics of peak cluster-depression karstic terrains in Southwest China (Fig. 1) (Qin et al., 2020a). In the hills, calcareous soils develop from dolomite and limestone and correspond to Mollic Inceptisols (Liu et al., 2020; Zhao et al., 2010). The valley depressions are mainly covered with quaternary soils which were transported and deposited from ambient hills (Liu et al., 2020). In general, soils are thicker (40-100 cm) in valley depressions than on hillslopes (mean < 50 cm) (Qin et al., 2020b) and consequently cropland mainly converges in valley depressions, occupying about 16.7% (2.8% for paddy and 13.9% for dry land) of this catchment area (Fig. 1) (Qin et al., 2020a). Scrub-grassland and deciduous broad-leaved forest, accounting for ~83.3% of the catchment area, mostly occur on the mountain regions. Approximately 64% of these natural vegetation types are recovered from abandoned cropland over the past decade (2006-2016). More details are described in the Supplementary Material (Text S1).

Under the regulation of a subtropical monsoon climate, the precipitation in the wet season (from May to October) of 2017 was more than six times that in the dry season (from November to April) (833 mm versus 137 mm). The recorded range in air temperature and humidity in 2017 both showed significant fluctuations, from -1.5°C to 36.6°C (mean 15.4 °C) and from 32.5% to 98.4% (mean 78.3%), respectively.

<Fig. 1. Here>

After initial on-site assessment, four sampling sites with relatively symmetrical soil (thickness > 70 cm) and gentle terrain were selected that would most accurately represent four land-use types (Fig. 1), including cropland (CR), abandoned cropland (AC), shrub-grassland (SG) and secondary forest (SF). Site CR is characterized by *Zea mays* (May to Sep.) and *Brassica napus* (Oct. to Mar.) in rotation. Site AC is naturally recovered into shrub-grass land after farming cessation approximately a decade prior and is dominated by C3 plants (e.g., *Rhamnus davurica*, *Rubus biflorus*, and *Artemisia carvifolia*). Detailed information about dominant plants overlying the four sampling sites and corresponding $\delta^{13}C$ values of leaves (Fig. 2(b)) are referred to in previous publications (Du et al., 2014; Hao et al., 2019; Liu et al., 2020; Piao et al., 2001).

On April 18th, July 25th, September 20th and November 19th, 2017, a 50cm-diameter / 80 cm deep hole was excavated at each site. Soils were sampled from 0 cm (i.e., 0-5 cm surface soils collected after cleaning up overlying plant debris and detritus), 10 cm, 20 cm, 30 cm, 50 cm and 70 cm depth at each site for analyzing soil pH and C properties (including concentrations and isotopic compositions of both SOC and SIC). Soils for measuring moisture and bulk density were sampled using the cutting ring method at the corresponding depth (except 0 cm). Additionally, dominant rocks at AC, SG and SF were collected and ground into powder after cleaning the surface impurities for measuring the isotopic composition of inorganic C.

2.2. Sample measurements

All samples were pretreated and measured within 12 hours of collection. Soil moisture and soil bulk density were gravimetrically measured by drying soil (known weight) to a constant weight at 105°C. After eliminating visible plant residues and detritus and air-drying at 25°C, some soils were pulverized and passed through an 80-mesh sieve to measure pH in a mix of soil and water (1:2.5) (Liu et al., 1996). The remaining soils were divided into two parts after being ground and passed through a 100-mesh sieve. For rock isotopic determination, one part of the powdered samples were directly put into glass bottles containing a magnetic stir bar before applying a vacuum and injecting with diluted phosphoric acid, to convert all inorganic

C into CO_2 by stirring at 50 °C for 12 hours (Cui et al., 2013). Another part was further acidified with HCl (0.5 mol L^{-1}) for 24 hours to remove inorganic C (Midwood and Boutton, 1998), washed to neutrality using distilled water, dried at 60°C to a constant weight, and then pulverized and passed through a 100-mesh sieve. After that, subsamples were combusted at 850°C for 2 hours in sealed quartz tubes containing CuO, to convert SOC into CO_2 for measuring isotope compositions (Boutton, 1991; Zhu et al., 2005). CO_2 for isotope analysis was all subsequently extracted and purified cryogenically on the vacuum line. $^{13}C/^{12}C$ (R) were measured by an Isotope Ratio Mass Spectrometer (IRMS; Thermo, 253 Plus) and reported using the delta (δ) notation in per mil (‰) relative to a standard (V-PDB) as follows, with an accuracy of ± 0.1‰:

$$\delta^{13}C(‰) = (R_{sample}/R_{standard} - 1) \times 10^3 \qquad (1)$$

Other subsamples were used to measure SOC concentrations ([SOC]) with an elemental analyzer (Vario MAX CNS analyzer, Elementar Analysensysteme, Hanau, Germany). SIC concentrations ([SIC]) were obtained from the difference between soil weight before and after removing inorganic C after considering the mole fraction of C in $CaCO_3$ (0.12), as most SIC exist in the form of carbonate minerals (Wu et al., 2009). This method may slightly overestimate [SIC] as acidification treatment can cause other soluble matter loss in addition to carbonates. But these constituents should make negligible contribution to this difference value and the resultant uncertainty should be acceptable, as [SIC] estimated by this calculation corresponds to the volume of CO_2 used for measuring $\delta^{13}C$ of SIC. Soil total carbon (STC) is defined as the sum of SIC and SOC.

2.3. Data analyses and statistics

SIC and SOC stocks in each soil layer were estimated using the following equations (Wu et al., 2003):

$S_{SIC} = [SIC] \times \rho \times (1 - f_s) \times \Delta D \times 10^{-2}$ (2)

$S_{SOC} = [SOC] \times \rho \times (1 - f_s) \times \Delta D \times 10^{-2}$ (3)

where: S_{SIC}/S_{SOC} and [SIC]/[SOC] refer to stocks (kg m^{-2}) and concentrations (g kg^{-1}) of SIC/SOC, respectively; ρ, f_s and ΔD refer to the soil bulk density (g cm^{-3}), the volumetric proportion of non-soil fragment of > 2 mm diameter (dimensionless) and the thickness of soil layer (cm). In this study, f_s is assumed to be zero as there is almost no particles with > 2 mm diameter in whole soil profiles. The soil total carbon stock (S_{STC}) in each soil layer is the sum of S_{SIC} and S_{SOC}.

The decomposition of SOC and the enrichment of ^{13}C in the remainder were calculated by the Rayleigh equation (Accoe et al., 2002):

$\delta^{13}C_{SOC} = a + \varepsilon \ln(C/C_0)$ (4)

where: C and C_0 refer to [SOC] corresponding to $\delta^{13}C_{SOC}$ and the highest [SOC] in the surface soil (0cm) of individual land uses, respectively, a is the constant which approximately equals the $\delta^{13}C_{SOC}$ corresponding to C_0, ε is the enrichment factor.

The proportions of "new" carbon (f_{new}, %) and "old" carbon (f_{old}, %) in SOC in AC topsoil were reckoned by the following isotopic mass balance equation (Del Galdo et al., 2003):

$f_{new} = (\delta^{13}C_{AC} - \delta^{13}C_{CR}) / (\delta^{13}C_{VE} - \delta^{13}C_{CR}) \times 100$ (5)

$f_{old} = 100 - f_{new}$ (6)

where: $\delta^{13}C_{CR}$ and $\delta^{13}C_{AC}$ denote $\delta^{13}C_{SOC}$ in CR and AC, respectively. $\delta^{13}C_{VE}$ is the average $\delta^{13}C$ of leaves of overlying dominant vegetation in AC, which is calculated to be -28.5±0.7‰ after referring to Du et al. (2014).

The decomposition rate constant (k) of SOC and the increasing rate (v) of "new" SOC in AC were estimated by the following equations (Marin-Spiotta et al., 2009):

$$k = -\ln(C_t/C_0) / t \qquad (7)$$

$$v = d / t \qquad (8)$$

where: t, C_0, C_t and d denote time (yr) since ceasing farming, the SOC stock (taking the value in CR as reference, kg m^{-2}) before ceasing farming, the remaining "old" SOC stock (kg m^{-2}) and the increment of "new" SOC (kg m^{-2}) after ceasing farming for t years, respectively.

The percentages of lithogenic and pedogenic carbonates in SIC in diverse soil layers were calculated based on the following mass balance (Landi et al., 2003):

$$f_P = (\delta^{13}C_{SIC} - \delta^{13}C_L) / (\delta^{13}C_P - \delta^{13}C_L) \times 100 \qquad (9)$$

$$f_L = 100 - f_P \qquad (10)$$

where: f_P and f_L denote the percentage of pedogenic component and lithogenic component in SIC, respectively. The intercept of linear fitting between [SIC] and $\delta^{13}C_{SIC}$ was assumed as $\delta^{13}C_P$ (the $\delta^{13}C$ of pedogenic carbonate) in the corresponding land use. The $\delta^{13}C$ of dominant rocks (1.0 ± 0.1‰) was assumed as $\delta^{13}C_L$ (the $\delta^{13}C$ of lithogenic carbonate). The stock of lithogenic component (S_L) and pedogenic component (S_P) can be calculated according to f_P, f_L and SIC stocks.

Data was analyzed using a combination of one-way ANOVA and Multiple regression analysis. The details and results of statistical analyses are given in the Supplementary Material (Texts S2 and S3).

3. Results

3.1 Soil physicochemical properties

Soil moisture (w) varied between 20.2% and 45.0% with a coefficient of variation (CV) of 17.2%. It showed significant differences ($P < 0.05$) among diverse depths of individual profiles and among different land uses (Fig. S1 (a)). Soil bulk density (ρ) was negatively correlated with w ($R^2 = 0.6$, $P < 0.001$), ranging from 1.0 to 1.6 g cm^{-3} (CV=9.7%) (Fig. S1 (b)). Soil pH were mostly between 6 and 7 (CV=5.8%) (Fig. S1 (c)), averaging 6.2±0.4 at CR, 6.5±0.3 at SF, 6.6±0.3 at AC, and 6.7±0.3 at SG. The C/N ratio (r) in soil organic matter varied from 5.2 to 17.0 (CV=22.6%) and generally decreased with increasing depth except at site CR (Fig. S1 (d)). Most soil profiles showed significant seasonal variation ($P < 0.05$) for w, pH and r but not for ρ (Fig. S2).

3.2. Soil carbon characteristics

[SOC] ranged from 7.0 to 119.3 g kg^{-1} (mean 26.8±18.5 g kg^{-1}) and decreased with increasing depth (Fig. 2 (a)). The mean [SOC] followed the order of SF (86.4 ± 32.4 g kg^{-1}) > SG (66.0 ± 18.0 g kg^{-1}) > AC (49.9 ± 15.4 g kg^{-1}) > CR (27.9 ± 0.2 g kg^{-1}) in topsoil but approached uniform values (~10 g kg^{-1}) across all sites in the subsoil. The $\delta^{13}C$ of SOC ($\delta^{13}C_{SOC}$) varied from -27.3‰ to -19.4‰ (mean -22.4 ± 1.5‰). As depth increases, $\delta^{13}C_{SOC}$ firstly increased in the 0-20 cm layer but then slowly decreased from 20-70 cm (Fig. 2 (b)). Both

[SOC] and $\delta^{13}C_{SOC}$ showed significant differences in vertical profiles and in land uses (Fig. 2 (a) and (b)) but not in seasonal variations (Fig. 3 (a) and (b)).

<Fig. 2. Here>

<Fig. 3. Here>

[SIC] in this study was significantly lower than [SOC] ranging from 0.4 to 3.5 g kg^{-1} (mean 1.4±0.7 g kg^{-1}), higher at SF and SG but lower at CR. It increased with increasing depth in general, except at SG where [SIC] decreased in the 0-30 cm layer (Fig. 2 (c)). The $\delta^{13}C$ of SIC ($\delta^{13}C_{SIC}$) were between -20.4‰ and -3.0‰ (mean -13.7±4.3‰) and had similar changes with depth as [SIC] (Fig. 2 (d)). There was no significant seasonal difference in both [SIC] and $\delta^{13}C_{SIC}$ for all land-use types observed (Fig. 3 (c) and (d)).

The S_{SOC} in the 0-70 cm soil layers varied from 15.6 to 25.2 kg m^{-2} (CV=12.6%), averaging 18.4±1.8 kg m^{-2} at SG, 19.7±0.9 kg m^{-2} at CR, 20.1±2.9 kg m^{-2} at SF, and 22.9±1.6 kg m^{-2} at AC. Over 50% of the SOC was distributed in the 0-30 cm soil layer (Fig. 4 (a)). The S_{SIC} in the 0-70 cm soil layers ranged from 0.7 to 2.0 kg m^{-2} and accounted for less than 10% (mean 6.0 ± 3.7%) of S_{STC} stock in most soil profiles (Fig. 4 (b) and (c)), averaging 0.8±0.1 kg m^{-2} at CR, 1.0±0.1 kg m^{-2} at AC, 1.5±0.2 kg m^{-2} at SF, and 1.6±0.4 kg m^{-2} at SG. Over 50% of the SIC was stored in the 30-70 cm soil layer (Fig. 4 (b)). The vertical variations of S_{STC} in individual soil profiles were comparable to that measured in S_{SOC} (Fig. 4 (c)). Since similar soils are considered to have similar processes of C accumulation (Bai and Zhou, 2020), the soil C amount in the 0-70cm soil layer of this catchment could be roughly calculated based on C stocks and areas of various land uses, at 27.9×10^3 t, including 26.5×10^3 t of SOC and 1.4×10^3 t of SIC (Table 1). Although these values might be overestimated as the calculation process did not consider the area of other land uses (e.g., developed areas and bare rock), this potential uncertainty should be acceptable as the sum area of these neglected land uses accounts for less than 1% in this catchment (Qin et al., 2020b; Yue et al., 2020).

<Fig. 4. Here>

<Table 1. Here>

4. Discussions

4.1. Vertical variations of SOC in karst regions

The vertical variations of SOC in this study have also been observed in other regions (Table 2) and are likely due to any or a combination of the following: (1) abundant plant residues in the topsoil; (2) less vegetal roots and their exudates in the subsoil (Ni et al., 2015); (3) limited microorganism activity and organic matter (OM) supplementation in the subsoil. The coupled vertical characteristics of [SOC] and $\delta^{13}C_{SOC}$ likely reflect microbial decomposition processes. During OM decomposition, ^{12}C is utilized preferentially by microorganisms and released as gas (e.g., CO_2 and CH_4), with the remaining ^{13}C-enriched portion being assimilated into microbial biomass and transformed into the SOC pool (Poage and Feng, 2004). Higher degrees of decomposition thus could cause more ^{13}C enrichment in the residual OM, leading to an increase in $\delta^{13}C_{SOC}$ with increasing depth, potentially of greater significance in the 0-20 cm profile where labile organic C sources and associated microbiota may be more prolific. Additionally, roots which are mainly distributed in the 0-20 cm layers are more ^{12}C-depleted than leaves or twigs above (Hao et al., 2019), leading to higher $\delta^{13}C_{SOC}$ in rhizosphere soil than in surface soil. Another potential explanation is the continued decline of the $\delta^{13}C$ of atmospheric CO_2 since the industrial revolution (Cuntz, 2011), SOC formed later thus could inherit isotopically lighter C from overlying vegetation than that formed earlier. In deeper soils (< 20 cm), however, the slight downtrend of $\delta^{13}C_{SOC}$ may be caused by (1) the accumulation of lignin and lipids (Benner et al., 1987); (2) the downward migration of colloidal organic C (Becker-Heidmann and Scharpenseel, 1992); and / or (3) the contribution from mineral-associated organic C existing in bedrocks (Liu et al., 2020).

<Table 2. Here>

The observed relationships between [SOC] and $\delta^{13}C_{SOC}$ of all land uses were well characterized by Rayleigh equations (Fig. 5 (a)), but this only occurs in the 0-20 cm soil layers and not in soils below 20 cm. This indicates that fresh SOC in Chenqi catchment are mostly active within surface soil layers, and the variation mechanism of SOC is discrepant across the whole individual profile. One possible reason for this is that the labile SOC pool, which has a relatively short turnover time and high activity, is mostly present in topsoil (Ellert and Janzen, 2006; McLauchlan and Hobbie, 2004; Wu et al., 2003). With increasing depth, however, SOC pool tends to higher recalcitrance and gradually approaches predominantly mineral horizons where microbial activity weakens and SOC has a much longer turnover time (≥ 100~1000 years) (Wu et al., 2003). Forming 1 cm of soil in the K-CZ takes more than 10^4 years on average (Liu et al., 2016; Wei, 1996), and most “fresh” organic C inputting into the soil scarcely migrate down into deeper “old” soils (Ellert and Janzen, 2006; Yu et al., 2019). Deeper “old” soils that undergo minimal disturbance may have reached equilibrium and well retain early characteristics which cannot be readily altered without substantially changing the soil structure.

<Fig. 5. Here>

4.2. Impacts of land uses on SOC

The differences in [SOC] among four sampling sites indicate the control of land uses and the negative impact of farming activities on [SOC], especially in the surface cultivated layers. Firstly, the limited input of OM in agricultural soils is almost exclusively from periodic farming activities (e.g., fertilization). Besides, frequent cultivation and plowing can reduce the vertical heterogeneity of cultivated soil layers (Li et al., 2016a), increase the possibility of soil exposure, and make for SOC consumption through boosting mineralization and decomposition rates (Schjønning and Thomsen, 2013). Moreover, water erosion in cropland soils can significantly enhance material loss and reduce soil fertilities (Lizaga et al., 2018). The leaching process and reduced replenishment of soil cations (e.g., calcium and magnesium) in cropland can also lower soil pH and subsequently weaken metal-humus complexation (Li et al., 2017).

In contrast, at sites SF and SG, more plant residues (e.g., fallen leaves and deadwood) from overlying natural vegetations can keep providing soils with OM. A well-developed root system of the overlying plant communities can also improve soil and water conservation and subsequently reduce OM losses (Sun et al., 2015). Moreover, the two sites are located on hillsides covered with calcareous soils, in which calcium and magnesium can combine with humus decomposed from OM, forming condensed and stable humus calcium (Heckman et al., 2009). Accordingly, [SOC] and its spatio-temporal variations are both lower in CR than at other non-farming sites. It is noteworthy that altitude and altitude-involved factors can also cause difference in SOC between sampling sites, like the impact of solar insolation on SOC mineralization (Bai and Zhou, 2020; Wu et al., 2003). However, while care was taken to maximize altitude similarity, the variability of this karst catchment characteristics (e.g., area, soil thickness, and the vertical distribution of natural vegetation) yields a small but non-zero altitude difference among the four sampling sites, and consequently may be of minor influence.

Theoretically, compared to cropland, non-farming land with a natural vegetation cover generally has higher microbial biomass and associated enzymatic activities (Ni et al., 2015). The resultant faster decomposition and turnover rates could be expected to elevate the degree of C isotopic fractionation and lead to a greater increment for $\delta^{13}C_{SOC}$ in upper soil layer. In this study, however, the absolute value of the enrichment factor (ε) in the Rayleigh equation follows the order of AC (4.8) > SG (4.3) > CR (2.6) > SF (2.4) (Fig. 5 (a)). This is counter to our expectation that the highest ε value would occur in SF. Moreover, the mean Δ[SOC] (change of [SOC] per depth increment) in the 0-20 cm layer follows the order of SF (3.00 g kg^{-1} cm^{-1}) > SG (1.85 g kg^{-1} cm^{-1}) > AC (0.90 g kg^{-1} cm^{-1}) > CR (0.34 g kg^{-1} cm^{-1}), which is inconsistent with $\Delta\delta^{13}C_{SOC}$ (change of $\delta^{13}C_{SOC}$ per depth increment) which follows the order of SG (0.18 ‰ cm^{-1}) > AC (0.15‰ cm^{-1}) > SF (0.13‰ cm^{-1}) > CR (0.04‰ cm^{-1}). The discordances of both ε and Δ among different land uses indicate that in the thin and heterogeneous karst soils, there are other factors (e.g., substrate availabilities) affecting enrichment efficiency of ^{13}C in addition to vegetation coverage. Isotope fractionations in karst soil profiles are not completely consistent with the turnover rate of SOC, which is possibly regulated by size of soil aggregates and species of aboveground vegetation and belowground microbial communities (Liu et al., 2020; Martí-Roura et al., 2019).

Long-term farming activities have been shown to lower the background level of SOC (Li et al., 2016a). Intensive tillage can break macroaggregates (250-2000μm) which dominate soil aggregation and partly control SOC stability, enabling the protected organic C within macroaggregates to be exposed and decomposed or mineralized more readily (Six et al., 2000). After ceasing farming, high mineralization of SOC during the farming period may limit the initial accumulation of "new" SOC (Martí-Roura et al., 2019), affecting the expected SOC improvement of agricultural abandonment. Evidence shows it may take longer to improve active SOC and restore soil fertilities until the structure and function of soil and vegetation are gradually reestablished (Li et al., 2016b; Post and Kwon, 2000). The dynamic equilibrium between SOC formation and OM decomposition can often not be reached over a short time (Liu et al., 2020; Schlesinger, 1977).

The higher S_{SOC} in AC than in CR (Fig. 4 (a)) implies that ceasing cultivation can relieve the on-going loss of SOC and help maintain / improve soil quality, especially in the topsoil. In the tenth year after ceasing ploughing in AC, f_{new} was calculated to be 34 ± 10% in 0-10 cm layer but close to 0% in the deeper layers, denoting that during the first decade after abandoning farming, some "new" OM imported into soil could been retained, but the natural restoration mainly occurs within topsoil, namely the "young pool" proposed by Ellert and Janzen (2006). The v and k of SOC in AC were calculated to be 0.18 kg m^{-2} yr^{-1} and 0.01, respectively, reflecting that the incipient (the first decade) effect of agricultural abandonment is better in this karst catchment than in the hinterland of the Loess Plateau (v = 0.11 kg m^{-2} yr^{-1}; k = 0.04) (Deng et al., 2016). In karst regions, macroaggregates in topsoil can recover rapidly (Liu et al., 2020)and the lost calcium caused by long-term tillage can also be rapidly replenished from the limestone dissolution after farming cessation, stabilising SOC (Li et al., 2017). The functional bacteria involved in C fixation might be more active and diverse in karst soils (Tong et al., 2021). Additionally, dissolved organic C in surface runoff may be partially withheld or adsorbed during percolation processes, contributing further to the SOC pool (Qin et al., 2021). Therefore, the effect of agricultural abandonment on SOC may be better in karst systems with their unique hydrogeology than in non-karst regions. Although this karst catchment has a higher S_{SOC} (15.6~25.2 kg m^{-2}) than the average level recorded in China (8.0 kg m^{-2}) and globally (10.6 kg m^{-2}) (Post et al., 1982; Wu et al., 2003), the availability of SOC and whether the effect of natural restoration or artificial afforestation is better require further study to seek the most efficient and economical managements for sequestering C and recovering soil fertility in agricultural karst soils.

4.3. Vertical dynamics of SIC in karst regions

The vertical distribution of [SIC] is opposite to [SOC] variation in this study, which is in line with observation in some other regions (Table 2), such as the foothill Himalayas (Hussain et al., 2019), Qinghai Lake basin (Li et al., 2016a), and Xilin River basin (Wang et al., 2013), reflecting that the soil condition in these regions might be more favorable for the negative impact of SOC on SIC vertical variations. The results of multiple regression analysis suggest that SOC variation could affect [SIC] and $\delta^{13}C_{SIC}$ (Text S3). SOC accumulation can increase carbonic and organic acid levels and subsequently decrease SIC by lowering the availability of Ca^{2+} and elevating the dissolution and leaching of carbonates (Sartori et al., 2007). SOC decomposition can also produce CO_2 and subsequently increase SIC by facilitating the development of authigenic carbonates (Kolesár and Čurlik, 2015). This potential impact of SOC on SIC in karst soils might also be attributable to its specific properties of thin soil layers, high permeability, and intense carbonate weathering, which can affect microbial activities and the availability of critical reactants (e.g., Ca^{2+}, soil CO_2 and H_2O) for forming authigenic carbonates. In contrast, a similar vertical trend between [SIC] and [SOC] was observed in the Mediterranean area and Chinese Loess Plateau, where [SIC] is significantly higher than [SOC] (Martí-Roura et al., 2019; Yu et al., 2020). This phenomenon was attributed to the combination of OM with high calcium contents in these regions, thus high SIC favors SOC accumulation by providing physicochemical protection from breakdown within formed macroaggregates (Martí-Roura et al., 2019). Accordingly, the role of SOC in SIC vertical variation is likely to be regulated by regional soil properties (e.g., soil pH, soil development and parent materials, and the availability of reactants) and meteorological factors (e.g., rainfall and temperature) at a larger scale. The possible negative influence of SOC on SIC in this, and potentially other karst regions warrants more in-depth investigation.

The $\delta^{13}C_{SIC}$ in this study are more negative than observed on the Chinese Loess Plateau (Cui et al., 2013), the northern margin oasis of the Tarim Basin (Li et al., 2018), and many regions globally (e.g., The Netherlands, Alaska and Saskatchewan) (Cerling, 1984; Fischer-Femal and Bowen, 2021). We thus speculate that there is an active SIC-CO_2-SOC system and a fast C cycle in karst soils. Karst catchments of SW China are generally characterized by plentiful rainwater, high permeability, high sensitivity to environmental factors, and intense carbonate weathering (Yuan and Zhang, 2008; Zhang et al., 2021). These conditions could elevate microbial activity and accelerate the circulation of CO_2 and the combination between organic C and inorganic C under appropriate oxygen conditions (Cerling, 1984; Li et al., 2016a; Martí-Roura et al., 2019). These specific karst structures and resultant modern biological processes are more likely to lower $\delta^{13}C$ of soil CO_2 through continuous exchange (Cerling, 1984; Clark and Fritz, 1997), generating new C sequestration alongside a potentially unstable C pool. Moreover, ^{13}C-depleted biogenic CO_2 can combine with abundant calcium and magnesium and form "fresh" carbonates within soils (Landi et al., 2003; Yao et al., 2010). Overall, the long-term dynamic equilibrium of soil respiration, carbonate dissolution and reprecipitation controls [SIC] and $\delta^{13}C_{SIC}$, becoming a key link in the C cycle in karst soils. Although the S_{SIC} (0.7~2.0 kg m^{-2}) in this karst catchment is lower than the average level in China (6.2 ± 1.2 kg m^{-2}) (Wu et al., 2009), the SIC pool is more and labile and readily cycled in thin karst soils due to readily available Ca^{2+}, soil CO_2 and H_2O. It thus cannot be ignored when investigating SOC dynamics within karst soils and evaluating the C sink in karst zones and its role in global C budgets.

4.4. Impacts of land uses on SIC

In this study, the lower S_{SIC} in CR than in SG and SF (Fig. 4 (b)) indicates that long-term farming activates potentially cause SIC losses. Generally, SIC variation is directly controlled by artificial disturbance, ambient conditions, and some physical and chemical reactions (Li et al., 2015; Xu et al., 2019). In cropland, especially in soils with acidic fertilizer application, excessive fertilization would promote SIC loss (Perrin et al., 2008), where irrigation can also accelerate vertical leaching of carbonates into deeper soil layers (Sartori et al., 2007). Specifically, tillage benefits carbonate weathering by exposing the calciferous horizon to the external environment (Lal and Kimble, 2000), and long-term ploughing would narrow the profile differences of [SIC] by mixing (Li et al., 2016a). Additionally, soil pH and pH-involved processes will affect SIC dynamics (Li et al., 2016a; Shi et al., 2012), with acidic conditions increase the risk of SIC losses. These provide explanations for why the lowest [SIC] and its CV both occurred in CR. Wu et al. (2009) also found that SIC losses mostly occur in cultivated soils and are mainly related to climate. In contrast, Quijano et al. (2020) found that [SIC] in the Mediterranean Calcisols, where soils are alkaline (pH>7), was higher in cultivated land than in uncultivated land. This observation was attributed to the distribution and precipitation of different sized particles in soils. Accordingly, land uses can affect SIC variation, but the related controlling factors differ between regions.

SIC includes a lithogenic component (primary carbonates) and a pedogenic component (secondary carbonates) (Wu et al., 2009). In this study, both lithogenic and pedogenic stocks (S_L and S_P) were generally higher in the subsoil than in topsoil in most soil profiles (Fig. 6 (a)), suggesting that the two components in topsoil are both likely to be lost. Appropriate circumstances (like high soil moisture) favor carbonate dissolution in upper soil layers, causing the calcic horizons to migrate down (Wu et al., 2009). The subsequent reprecipitation in subsoils resulting from adequate reactants (e.g., Ca^{2+}, soil CO_2 and H_2O) can increase the pedogenic stock. The mean f_P was calculated to be 67.5 ± 15.9%, and over 80% of soil samples had a f_P > 55% (Fig. 6 (b)). This result is in line with some other reports (Li et al., 2016a; Wu et al., 2009), demonstrating that pedogenic carbonates dominate SIC stocks and largely control SIC variation. In this karst catchment, dissolved inorganic C in spring water is mostly derived from biogenic CO_2 instead of primary carbonates (Qin et al., 2020b), this can indirectly reflect the relative stability of lithogenic SIC and the favorable condition for the dissolution and reprecipitation of pedogenic carbonates (i.e., the availability of biogenic CO_2 and Ca^{2+} in soil). Additionally, f_P and f_P/f_L both increased with decreasing depth in CR and AC (Fig. 6 (b) and (c)). This probably further means that during the loss processes of the two SIC components, cultivation condition is more conducive to the occurrence of dissolution and reprecipitation in the upper cultivated layers, eventually elevating the relative proportion of the pedogenic component in SIC.

For other land-use types without artificial disturbance, the vertical distribution of SIC is more likely to be a result of natural accumulation processes. In these cases the higher SIC in subsoil than in topsoil is probably ascribed to the effect of the weathering of carbonate bedrocks. The intense carbonate weathering at the rock-soil interface provides adequate reactants (e.g., Ca^{2+}) for carbonate reprecipitation in the soil. This effect is particularly obvious at the hillslope of SF (Fig. 6), where the soil is relatively thin.

<Fig. 6. Here>

In soil profiles, vegetal roots and their exudates, and microbial activity and biomass normally present an uneven distribution (higher in upper layer than in lower layer) (Liu et al., 2020; Ni et al., 2015). The impacts exerted by them on the SIC pool are thus expected to differ in different depths. However, [SIC] and $\delta^{13}C_{SIC}$ showed a positive linear correlation in the 0-20 cm soil layer and this trend was generally consistent with that in 20-70 cm layer for each land use type (Fig. 5 (b)), which differs significantly from SOC. This reflects the different variation mechanisms between SIC and SOC, and it may also indicate that the direct influence of biological factors on SIC dynamics should be weaker than on SOC. The regression slope between [SIC] and $\delta^{13}C_{SIC}$ follows the order of CR (12.2) > AC (8.2) > SG (3.1) > SF (2.0), and [SIC] fluctuates more narrowly in CR profiles (Fig. 5 (b)), reflecting the strong response of $\delta^{13}C_{SIC}$ to [SIC] variation in CR. This might support the conclusion that agricultural activities are more likely to alter the relative ratios of lithogenic SIC to pedogenic SIC.

Overall, the characteristics of karst regions, such as thin soil layer, high hydrological sensitivity, and intense carbonate weathering, have the potential to provide adequate reactants (e.g., Ca^{2+}, soil CO_2 and H_2O) for forming pedogenic SIC, especially at the rock-soil interface in hillslopes covering thinner soil and natural vegetation. Additional agricultural disturbances in valley depression can seemingly increase the relative proportion of pedogenic component in SIC in upper cultivated layers.

5. Conclusions

This study investigated concentrations and isotopic compositions of both SOC and SIC in different depths of four land-use soil profiles at a typical karst region, SW China. The results showed that the fresh SOC is mostly active in topsoil where its variation mechanism differs from subsoil under karst conditions (e.g., thin soils, high perviousness, and intense carbonate weathering). In contrast, The vertical heterogeneity of SIC and the direct influence of biological factors on SIC are both weaker relative to SOC. Additionally, the vertical variations of SOC and SIC are both susceptible to land-use change in karst zones. Farming activities can facilitate both SOC and SIC losses from karst soils, which can be alleviated or even partially restored after agricultural abandonment. The incipient natural restoration of SOC after ceasing tillage mainly occurs (at least initially) within topsoil where "new" carbon accounts for 34 ± 10% and the increasing rate of "new" SOC and the decomposition rate constant of SOC are 0.18 kg m^{-2} yr^{-1} and 0.01, respectively. SIC in karst soils are potentially more active and sensitive to land uses than in other landscapes, which is largely controlled by the dissolution and reprecipitation of pedogenic carbonate, especially in the upper cultivated layers. Overall, this study revealed an active SIC-CO_2-SOC system and a fast C cycle in karst zone soils where the dynamic exchange between and within the SOC and SIC pools might be crucial to better constrain their role in global C dynamics, especially in the context of expanding anthropogenic land use alteration. Further studies on water-soil interaction in karst regions are needed to clarify C sources and fate in the whole K-CZ.

Declaration of competing interest

The authors declare that they have no known competing financial interests or personal relationships that could have appeared to influence the work reported in this paper.

Acknowledgements

This work was supported by the Strategic Priority Research Program of Chinese Academy of Sciences [Grant number XDB40000000], and the National Natural Science Foundation of China [Grant number 41571130072, 41925002]. We are grateful to Susan Waldron and Quan Yuan for their valuable suggestions that greatly improved the quality of the manuscript. We thank Zhongjun Wang, Jie Zeng and Yucong Fu for their help in sample collections. We would also thank anonymous reviewers for their useful comments and Prof. Rumpel for guidance.

Appendix A. Supplementary material

Additional details on research region (Text S1), data analyses, statistics (Text S2) and results of multiple regression analysis (Text S3); additional 4 tables and 3 figures supporting results and discussions.

References

Accoe, F., Boeckx, P., Cleemput, O.V., Hofman, G., Zhang, Y., Li, R., Guanxiong, C., 2002. Evolution of the $\delta^{13}C$ signature related to total carbon contents and carbon decomposition rate constants in a soil profile under grassland. Rapid Commun Mass Spectrom 16(23), 2184-2189.

Bai, Y., Zhou, Y., 2020. The main factors controlling spatial variability of soil organic carbon in a small karst watershed, Guizhou Province, China. Geoderma 357, 113938.

Batjes, N.H., 1996. Total carbon and nitrogen in the soils of the world. European Journal of Soil Science 47(2), 151-163.

Battin, T.J., Luyssaert, S., Kaplan, L.A., Aufdenkampe, A.K., Richter, A., Tranvik, L.J., 2009. The boundless carbon cycle. Nature Geoscience 2(9), 598-600.

Becker-Heidmann, P., Scharpenseel, H.-W., 1992. Studies of soil organic matter dynamics using natural carbon isotopes. Science of the Total Environment 117-118, 305-312.

Benner, R., Fogel, M.L., Sprague, E.K., Hodson, R.E., 1987. Depletion of ^{13}C in lignin and its implications for stable carbon isotope studies. Nature 329(6141), 708-710.

Boutton, T.W., 1991. Stable carbon isotope ratios of natural materials, I. Sample preparation and mass spectrometric analysis. Carbon Isotope Techniques. Academic Press, New York, 155-171.

Campeau, A., Bishop, K., Amvrosiadi, N., Billett, M.F., Garnett, M.H., Laudon, H., Oquist, M.G., Wallin, M.B., 2019. Current forest carbon fixation fuels stream CO_2 emissions. Nature Communications 10(1), 1876.

Cerling, T.E., 1984. The stable isotopic composition of modern soil carbonate and its relationship to climate. Earth and Planetary Science Letters 71(2), 229-240.

Clark, I.D., Fritz, P., 1997. Environmental isotopes in hydrogeology. Lewis Publishers, New York.

Cui, L.-F., Liu, C.-Q., Tu, C.-L., Li, L.-B., Ding, H., 2013. Soil inorganic carbon and its isotopic composition under different vegetation types in Loess Plateau of Northwest China. Chinese Journal of Ecology 32(5), 1187-1194. (in Chinese)

Cuntz, M., 2011. Carbon cycle: a dent in carbon's gold standard. Nature 477, 547-548.

Davidson, E.A., Janssens, I.A., 2006. Temperature sensitivity of soil carbon decomposition and feedbacks to climate change. Nature 440(7081), 165-173.

Del Galdo, I., Six, J., Peressotti, A., Cotrufo, M.F., 2003. Assessing the impact of land-use change on soil C sequestration in agricultural soils by means of organic matter fractionation and stable C isotopes. Global Change Biology 9(8), 1204-1213.

Deng, L., Wang, K., Tang, Z., Shangguan, Z., 2016. Soil organic carbon dynamics following natural vegetation restoration: Evidence from stable carbon isotopes ($\delta^{13}C$). Agriculture, Ecosystems & Environment 221, 235-244.

Ding, H., Lang, Y.-C., Liu, C.-Q., 2016. Advances in study on leaching loss of carbon from soil. Earth and Environment 44(1), 139-146. (in Chinese)

Doetterl, S., Stevens, A., Six, J., Merckx, R., Van Oost, K., Casanova Pinto, M., Casanova-Katny, A., Muñoz, C., Boudin, M., Zagal Venegas, E., Boeckx, P., 2015. Soil carbon storage controlled by interactions between geochemistry and climate. Nature Geoscience 8(10), 780-783.

Du, X.L., Wang, S.J., Luo, X.Q., 2014. Effects of different soil types on the foliar $\delta^{13}C$ values of common local plant species in karst rocky desertification area in central Guizhou Province. Environmental Science 35(9), 3587-3594. (in Chinese)

Ellert, B.H., Janzen, H.H., 2006. Long-term biogeochemical cycling in agroecosystems inferred from ^{13}C, ^{14}C and ^{15}N. Journal of Geochemical Exploration 88(1-3), 198-201.

Eswaran, H., Van den Berg, E., Reich, P., Kimble, J., 1995. Global soil carbon resources. In:

Lal, R., Kimble, J., Levine, E., Stewart, B.A. (Eds.), Soils and Global Change. In: Advances in Soil Sci. CRC Press, Boca Raton, FL, pp. 27-44.

Falkowski, P., Scholes, R.J., Boyle, E., Canadell, J., Canfield, D., Elser, J., Gruber, N., Hibbard, K., Hogberg, P., Linder, S., Mackenzie, F.T., Moore, B., Pedersen, T., Rosenthal, Y., Seitzinger, S., Smetacek, V., Steffen, W., 2000. The global carbon cycle: A test of our knowledge of earth as a system. Science 290(5490), 291-296.

Fischer-Femal, B.J., Bowen, G.J., 2021. Coupled carbon and oxygen isotope model for pedogenic carbonates. Geochimica et Cosmochimica Acta 294, 126-144.

Ford, D., Williams, P., 2007. Karst Hydrogeology and Geomorphology. John Wiley & Sons., Chichester.

Friedlingstein, P., O'Sullivan, M., Jones, M.W., Andrew, R.M., Hauck, J., Olsen, A., Peters, G.P., Peters, W., Pongratz, J., Sitch, S., Le Quéré, C., Canadell, J.G., Ciais, P., Jackson, R.B., Alin, S., Aragão, L.E.O.C., Arneth, A., Arora, V., Bates, N.R., Becker, M., Benoit-Cattin, A., Bittig, H.C., Bopp, L., Bultan, S., Chandra, N., Chevallier, F., Chini, L.P., Evans, W., Florentie, L., Forster, P.M., Gasser, T., Gehlen, M., Gilfillan, D., Gkritzalis, T., Gregor, L., Gruber, N., Harris, I., Hartung, K., Haverd, V., Houghton, R.A., Ilyina, T., Jain, A.K., Joetzjer, E., Kadono, K., Kato, E., Kitidis, V., Korsbakken, J.I., Landschützer, P., Lefèvre, N., Lenton, A., Lienert, S., Liu, Z., Lombardozzi, D., Marland, G., Metzl, N., Munro, D.R., Nabel, J.E.M.S., Nakaoka, S.-I., Niwa, Y., O'Brien, K., Ono, T., Palmer, P.I., Pierrot, D., Poulter, B., Resplandy, L., Robertson, E., Rödenbeck, C., Schwinger, J., Séférian, R., Skjelvan, I., Smith, A.J.P., Sutton, A.J., Tanhua, T., Tans, P.P., Tian, H., Tilbrook, B., van der Werf, G., Vuichard, N., Walker, A.P., Wanninkhof, R., Watson, A.J., Willis, D., Wiltshire, A.J., Yuan, W., Yue, X., Zaehle, S., 2020. Global carbon budget 2020. Earth System Science Data 12(4), 3269-3340.

Hao, Z., Gao, Y., Ma, M., Green, S.M., Wang, J., Song, X., Dungait, J.A.J., Johnes, P.J., Xiong, B., Quine, T.A., Sun, X., Wen, X., He, N., 2019. Using $\delta^{13}C$ to reveal the importance of different water transport pathways in two nested karst basins, Southwest China. Journal of Hydrology 571, 425-436.

Heckman, K., Welty-Bernard, A., Rasmussen, C., Schwartz, E., 2009. Geologic controls of soil carbon cycling and microbial dynamics in temperate conifer forests. Chemical Geology 267(1-2), 12-23.

Houghton, R.A., 2007. Balancing the global carbon budget. Annual Review of Earth and Planetary Sciences 35(1), 313-347.

Hussain, S., Sharma, V., Arya, V.M., Sharma, K.R., Rao, C.S., 2019. Total organic and inorganic carbon in soils under different land use/land cover systems in the foothill Himalayas. Catena 182, 104104.

Jelinski, N.A., Kucharik, C.J., 2009. Land-use effects on soil carbon and nitrogen on a U.S. midwestern floodplain. Soil Science Society of America Journal 73(1), 217-225.

Jobbágy, E.G., Jackson, R.B., 2000. The vertical distribution of soil organic carbon and its relation to climate and vegetation. Ecological Applications 10(2), 423-436.

Kolesár, M., Čurlik, J., 2015. Origin, distribution and transformation of authigenic carbonates in loessic soils. Eurasian Journal of Soil Science 4(1), 38-43.

Lal, R., 2004. Soil carbon sequestration impacts on global climate change and food security. Science 304(5677), 1623-1627.

Lal, R., Kimble, J.M., 2000. Pedogenic carbonates and the global carbon cycle. In: Global climate change and pedogenic carbonates. Boca Raton:Lewis Publishers, 1-14.

Landi, A., Mermut, A.R., Anderson, D.W., 2003. Origin and rate of pedogenic carbonate accumulation in Saskatchewan soils, Canada. Geoderma 117(1-2), 143-156.

Lehmann, J., Kleber, M., 2015. The contentious nature of soil organic matter. Nature 528(7580), 60-68.

Li, C., Li, Q., Zhao, L., Ge, S., Chen, D., Dong, Q., Zhao, X., 2016a. Land-use effects on organic and inorganic carbon patterns in the topsoil around Qinghai Lake basin, Qinghai-Tibetan Plateau. Catena 147, 345-355.

Li, D., Wen, L., Yang, L., Luo, P., Xiao, K., Chen, H., Zhang, W., He, X., Chen, H., Wang, K., 2017. Dynamics of soil organic carbon and nitrogen following agricultural abandonment in a karst region. Journal of Geophysical Research: Biogeosciences 122(1), 230-242.

Li, Q., Chen, D., Zhao, L., Yang, X., Xu, S., Zhao, X., 2016b. More than a century of Grain for Green Program is expected to restore soil carbon stock on alpine grassland revealed by field ^{13}C pulse labeling. Science of the Total Environment 550, 17-26.

Li, Y.-M., Gong, L., An, S.-Q., Aun, L., Chen, X., 2018. Transfer of soil organic carbon to inorganic carbon in arid oasis based on stable carbon isotope technique. Environmental

Science 39(8), 3867-3975. (in Chinese)

Li, Y., Wang, Y.-G., Houghton, R.A., Tang, L.-S., 2015. Hidden carbon sink beneath desert. Geophysical Research Letters 42(14), 5880-5887.

Li, Z.P., Han, F.X., Su, Y., Zhang, T.L., Sun, B., Monts, D.L., Plodinec, M.J., 2007. Assessment of soil organic and carbonate carbon storage in China. Geoderma 138(1-2), 119-126.

Liu, C., Lang, Y., Li, S., Piao, H., Tu, C., Liu, T., Zhang, W., Zhu, S., 2009. Researches on biogeochemical processes and nutrient cycling in karstic ecological systems, southwest China: A review. Earth Science Frontiers 16(6), 1-12. (in Chinese)

Liu, C., Liu, Y., Guo, K., Zhao, H., Qiao, X., Wang, S., Zhang, L., Cai, X., 2016. Mixing litter from deciduous and evergreen trees enhances decomposition in a subtropical karst forest in southwestern China. Soil Biology and Biochemistry 101, 44-54.

Liu, G.S., Jiang, N.H., Zhang, L.D., Liu, Z.L., 1996. Soil physical and chemical analysis and description of soil profiles. China Standard Methods Press: Beijing, China, pp. 24-25. (in Chinese)

Liu, M., Han, G., Zhang, Q., 2020. Effects of agricultural abandonment on soil aggregation, soil organic carbon storage and stabilization: Results from observation in a small karst catchment, Southwest China. Agriculture, Ecosystems & Environment 288, 106719.

Lizaga, I., Quijano, L., Gaspar, L., Navas, A., 2018. Estimating soil redistribution patterns with ^{137}Cs measurements in a Mediterranean mountain catchment affected by land abandonment. Land Degradation & Development 29(1), 105-117.

Marin-Spiotta, E., Silver, W.L., Swanston, C.W., Ostertag, R., 2009. Soil organic matter dynamics during 80 years of reforestation of tropical pastures. Global Change Biology 15(6), 1584-1597.

Martí-Roura, M., Hagedorn, F., Rovira, P., Romanyà, J., 2019. Effect of land use and carbonates on organic matter stabilization and microbial communities in Mediterranean soils. Geoderma 351, 103-115.

McLauchlan, K.K., Hobbie, S.E., 2004. Comparison of labile soil organic matter fractionation techniques. Soil Science Society of America Journal 68(5), 1616-1625.

Mi, N.A., Wang, S., Liu, J., Yu, G., Zhang, W., JobbÁGy, E., 2008. Soil inorganic carbon storage pattern in China. Global Change Biology 14(10), 2380-2387.

Midwood, A.J., Boutton, T.W., 1998. Soil carbonate decomposition by acid has little effect on $\delta^{13}C$ of organic matter. Soil Biology and Biochemistry 30(10-11), 1301-1307.

Mishra, S.K., Gautam, S., Mishra, U., Scown, C.D., 2021. Performance-Based Payments for Soil Carbon Sequestration Can Enable a Low-Carbon Bioeconomy. Environmental Science & Technology 55(8), 5180-5188.

Moore, O.W., Buss, H.L., Green, S.M., Liu, M., Song, Z., 2017. The importance of non-carbonate mineral weathering as a soil formation mechanism within a karst weathering profile in the SPECTRA Critical Zone Observatory, Guizhou Province, China. Acta Geochimica 36(3), 566-571.

Ni, J., Luo, D.H., Xia, J., Zhang, Z.H., Hu, G., 2015. Vegetation in karst terrain of southwestern China allocates more biomass to roots. Solid Earth 6(3), 799-810.

Pain, A.J., Martin, J.B., Young, C.R., Valle-Levinson, A., Mariño-Tapia, I., 2020. Carbon and phosphorus processing in a carbonate karst aquifer and delivery to the coastal ocean. Geochimica et Cosmochimica Acta 269, 484-495.

Perrin, A.-S., Probst, A., Probst, J.-L., 2008. Impact of nitrogenous fertilizers on carbonate dissolution in small agricultural catchments: Implications for weathering CO_2 uptake at regional and global scales. Geochimica et Cosmochimica Acta 72(13), 3105-3123.

Piao, H.-C., Liu, Q.-M., Yu, D.-L., Guo, J.-H., Ran, J.-C., 2001. Origins of soil organic carbon with the method of natural ^{13}C abundance in maize fields. Acta Ecologica Sinica 21(3), 434-439. (in Chinese)

Poage, M.A., Feng, X., 2004. A theoretical analysis of steady state $\delta^{13}C$ profiles of soil organic matter. Global Biogeochemical Cycles 18(2), 1-13.

Post, W.M., Emanuel, W.R., Zinke, P.J., Stangenberger, A.G., 1982. Soil carbon pools and world life zones. Nature 298(5870), 156-159.

Post, W.M., Kwon, K.C., 2000. Soil carbon sequestration and land-use change: processes and potential. Global Change Biology 6(3), 317-327.

Pu, J., Jiang, Z., Yuan, D., Zhang, C., 2015. Some opinions on rock-weathering-related carbon sinks from the IPCC fifth assessment report. Advances in Earth Science 30(10), 1081-1090. (in Chinese)

Qin, C., Ding, H., Li, S.-L., Yue, F.-J., Wang, Z.-J., Zeng, J., 2020a. Hydrogeochemical Dynamics and Response of Karst Catchment to Rainstorms in a Critical Zone Observatory (CZO), Southwest China. Frontiers in Water 2(52), 577511.

Qin, C., Li, S.-L., Waldron, S., Yue, F.-J., Wang, Z.-J., Zhong, J., Ding, H., Liu, C.-Q., 2020b.

High-frequency monitoring reveals how hydrochemistry and dissolved carbon respond to rainstorms at a karstic critical zone, Southwestern China. Science of the Total Environment 714, 136833.

Qin, C., Li, S., Yue, F., Ding, H., Xu, S., Liu, C.-Q., 2021. Biogeochemical processes of dissolved carbon in the karst critical zone and its response to rainstorms. Quaternary Sciences 41(4), 1128-1139. (in Chinese)

Quijano, L., Kuhn, N.J., Navas, A., 2020. Effects of interrill erosion on the distribution of soil organic and inorganic carbon in different sized particles of Mediterranean Calcisols. Soil & Tillage Research 196, 104461.

Sartori, F., Lal, R., Ebinger, M.H., Eaton, J.A., 2007. Changes in soil carbon and nutrient pools along a chronosequence of poplar plantations in the Columbia Plateau, Oregon, USA. Agriculture, Ecosystems & Environment 122(3), 325-339.

Schjønning, P., Thomsen, I.K., 2013. Shallow tillage effects on soil properties for temperate-region hard-setting soils. Soil and Tillage Research 132, 12-20.

Schlesinger, W.H., 1977. Carbon balance in terresterial detritus. Annual Review of Ecology Evolution and Systematics 8(1), 51-81.

Schmidt, M.W., Torn, M.S., Abiven, S., Dittmar, T., Guggenberger, G., Janssens, I.A., Kleber, M., Kogel-Knabner, I., Lehmann, J., Manning, D.A., Nannipieri, P., Rasse, D.P., Weiner, S., Trumbore, S.E., 2011. Persistence of soil organic matter as an ecosystem property. Nature 478(7367), 49-56.

Shi, H.J., Wang, X.J., Zhao, Y.J., Xu, M.G., Li, D.W., Guo, Y., 2017. Relationship between soil inorganic carbon and organic carbon in the wheat-maize cropland of the North China Plain. Plant and Soil 418(1-2), 423-436.

Shi, Y., Baumann, F., Ma, Y., Song, C., Kühn, P., Scholten, T., He, J.S., 2012. Organic and inorganic carbon in the topsoil of the Mongolian and Tibetan grasslands: pattern, control and implications. Biogeosciences 9(6), 2287-2299.

Six, J., Elliott, E.T., Paustian, K., 2000. Soil macroaggregate turnover and microaggregate formation: a mechanism for C sequestration under no-tillage agriculture. Soil Biology and Biochemistry 32(14), 2099-2103.

Stockmann, U., Adams, M.A., Crawford, J.W., Field, D.J., Henakaarchchi, N., Jenkins, M., Minasny, B., McBratney, A.B., Courcelles, V.d.R.d., Singh, K., Wheeler, I., Abbott, L., Angers, D.A., Baldock, J., Bird, M., Brookes, P.C., Chenu, C., Jastrow, J.D., Lal, R., Lehmann, J., O'Donnell, A.G., Parton, W.J., Whitehead, D., Zimmermann, M., 2013. The knowns, known unknowns and unknowns of sequestration of soil organic carbon. Agriculture, Ecosystems & Environment 164, 80-99.

Sun, W., Zhu, H., Guo, S., 2015. Soil organic carbon as a function of land use and topography on the Loess Plateau of China. Ecological Engineering 83, 249-257.

Tong, H., Zheng, C., Li, B., Swanner, E.D., Liu, C., Chen, M., Xia, Y., Liu, Y., Ning, Z., Li, F., Feng, X., 2021. Microaerophilic Oxidation of Fe(II) Coupled with Simultaneous Carbon Fixation and As(III) Oxidation and Sequestration in Karstic Paddy Soil. Environmental Science & Technology 55(6), 3634-3644.

Wang, S.J., Liu, Q.M., Zhang, D.F., 2004. Karst rocky desertification in southwestern China:

geomorphology, landuse, impact and rehabilitation. Land Degradation & Development 15(2), 115-121.

Wang, X., Wang, J., Xu, M., Zhang, W., Fan, T., Zhang, J., 2015. Carbon accumulation in arid croplands of northwest China: pedogenic carbonate exceeding organic carbon. Scientific Reports 5, 11439.

Wang, Z.-P., Han, X.-G., Chang, S.X., Wang, B., Yu, Q., Hou, L.-Y., Li, L.-H., 2013. Soil organic and inorganic carbon contents under various land uses across a transect of continental steppes in Inner Mongolia. Catena 109, 110-117.

Wei, Q.F., 1996. Soil erosion in karst region of South China and its control. Research of Soil and Water Conservation 3(4), 72-76. (in Chinese)

Wu, H., Guo, Z., Gao, Q., Peng, C., 2009. Distribution of soil inorganic carbon storage and its changes due to agricultural land use activity in China. Agriculture, Ecosystems & Environment 129(4), 413-421.

Wu, H., Guo, Z., Peng, C., 2003. Distribution and storage of soil organic carbon in China. Global Biogeochemical Cycles 17(2), 1048.

Xu, X., Huang, Y., He, X., Wang, G., Su, Y., 2019. Effect of soil moisture and temperature on the soil inorganic carbon release of brown limestone soil in the karst region of Southwestern China. Environmental Science 40(4), 1965-1972. (in Chinese)

Yao, Z., Xiao, G., Wu, H., Liu, W., Chen, Y., 2010. Plio-Pleistocene vegetation changes in the North China Plain: Magnetostratigraphy, oxygen and carbon isotopic composition of pedogenic carbonates. Palaeogeography, Palaeoclimatology, Palaeoecology 297(2), 502-510.

Yu, X., Zhou, W., Chen, Y., Wang, Y., Cheng, P., Hou, Y., Wang, Y., Xiong, X., Yang, L., 2020. Spatial variation of soil properties and carbon under different land use types on the Chinese Loess Plateau. Science of the Total Environment 703, 134946.

Yu, X., Zhou, W., Cheng, P., Wang, Y., Hou, Y., Burr, G.S., Xiong, X., Wang, Y., Yang, L., Dodson, J., 2019. Soil organic carbon fractions and ^{14}C ages through 70 years of cropland cultivation. Soil and Tillage Research 195, 104415.

Yuan, D., Zhang, C., 2008. Karst dynamics theory in China and its practice. Acta Geoscientica Sinica 29(3), 355-365. (in Chinese)

Yue, F.J., Li, S.L., Waldron, S., Wang, Z.J., Oliver, D.M., Chen, X., Liu, C.Q., 2020. Rainfall and conduit drainage combine to accelerate nitrate loss from a karst agroecosystem: Insights from stable isotope tracing and high-frequency nitrate sensing. Water Research 186, 116388.

Zeng, S., Liu, Z., Kaufmann, G., 2019. Sensitivity of the global carbonate weathering carbon-sink flux to climate and land-use changes. Nature Communications 10(1), 5749.

Zhang, W., Wang, X., Lu, T., Shi, H., Zhao, Y., 2020. Influences of soil properties and hydrological processes on soil carbon dynamics in the cropland of North China Plain. Agriculture, Ecosystems & Environment 295, 106886.

Zhang, Z., Chen, X., Li, S., Yue, F., Cheng, Q., Peng, T., Soulsby, C., 2021. Linking nitrate dynamics to water age in underground conduit flows in a karst catchment. Journal of Hydrology 596, 125699.

Zhao, M., Zeng, C., Liu, Z., Wang, S., 2010. Effect of different land use/land cover on karst hydrogeochemistry: A paired catchment study of Chenqi and Dengzhanhe, Puding, Guizhou, SW China. Journal of Hydrology 388(1-2), 121-130.

Zhao, W., Zhang, R., Huang, C., Wang, B., Cao, H., Koopal, L.K., Tan, W., 2016. Effect of different vegetation cover on the vertical distribution of soil organic and inorganic carbon in the Zhifanggou Watershed on the loess plateau. Catena 139, 191-198.

Zhu, S., Liu, C., Tao, F., 2005. Use of $\delta^{13}C$ method in studing soil organic matter. Acta Pedologica Sinica 42(3), 495-503. (in Chinese)

Figures:

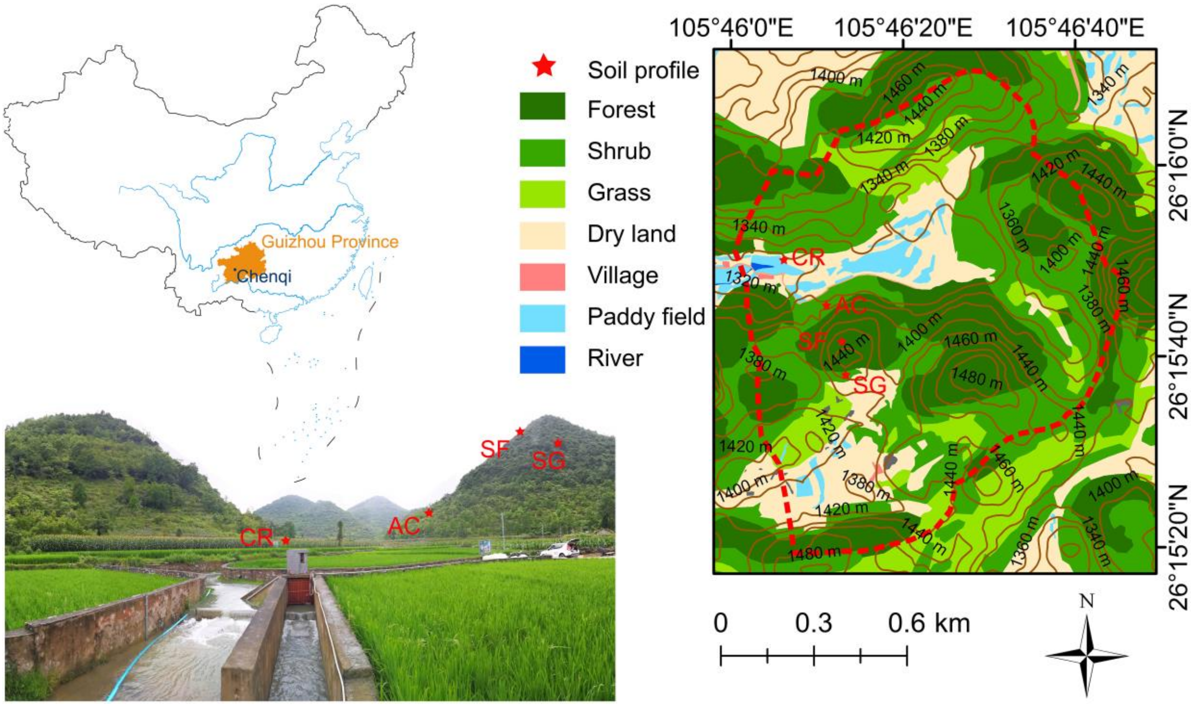

Figure 1: Location of the study area and sampling sites of four land uses, including cropland (CR), abandoned cropland (AC), shrub-grassland (SG) and secondary forest (SF).

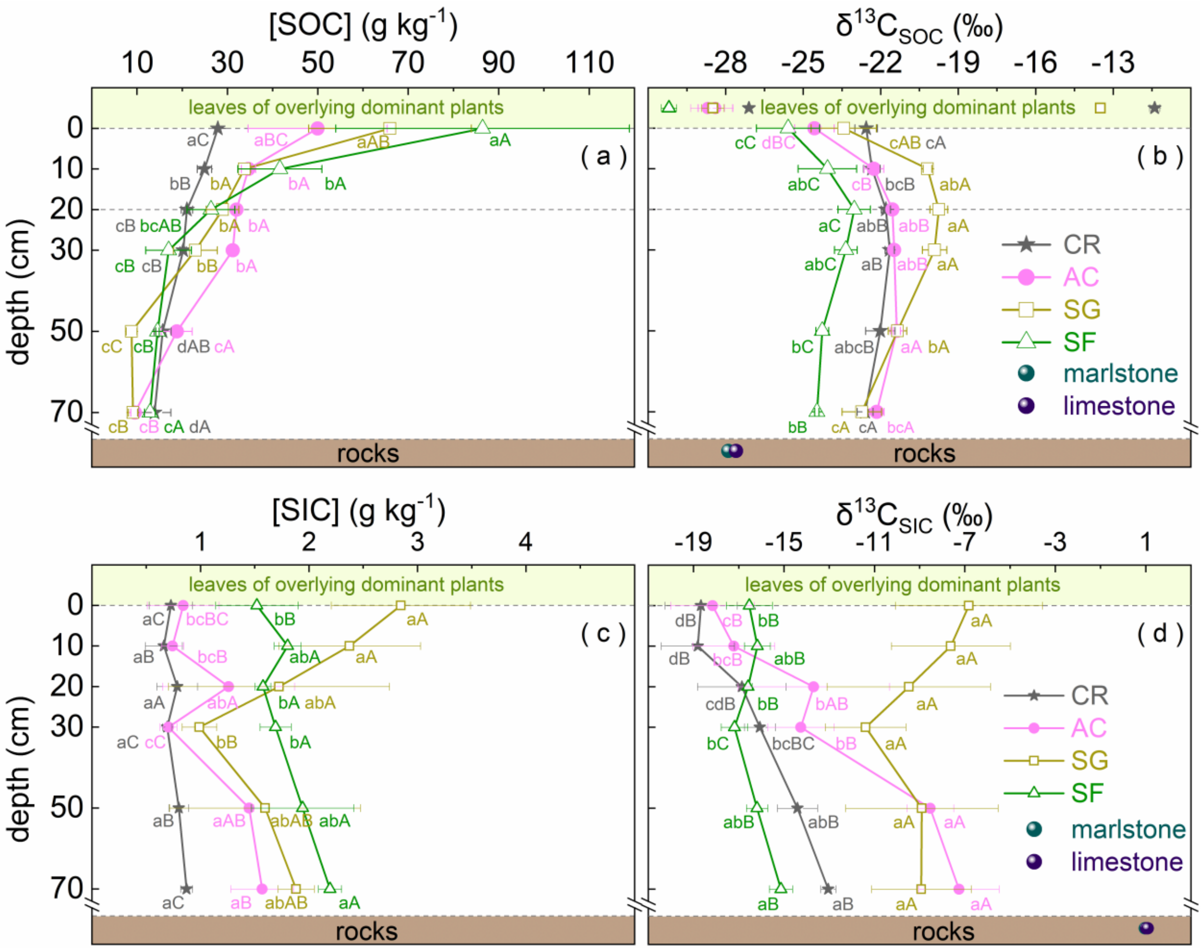

Figure 2: Vertical variations of [SOC] (a), δ13CSOC (b), [SIC] (c), and δ13CSIC (d) in four land-use soil profiles. Different lowercase letters and uppercase letters denote significant differences among diverse layer depth in the same land use and among diverse land uses in the same layer depth, respectively (one-way ANOVA, Duncan post-hoc test, $P < 0.05$). CR, AC, SG and SF refer to cropland, abandoned cropland, shrub-grassland and secondary forest, respectively. In panel (b), the δ13C values of organic carbon in bedrocks are referred to Liu et al. (2020), the δ13C values of leaves of overlying dominant plants are referred to publications (Du et al., 2014; Hao et al., 2019; Liu et al., 2020; Piao et al., 2001).

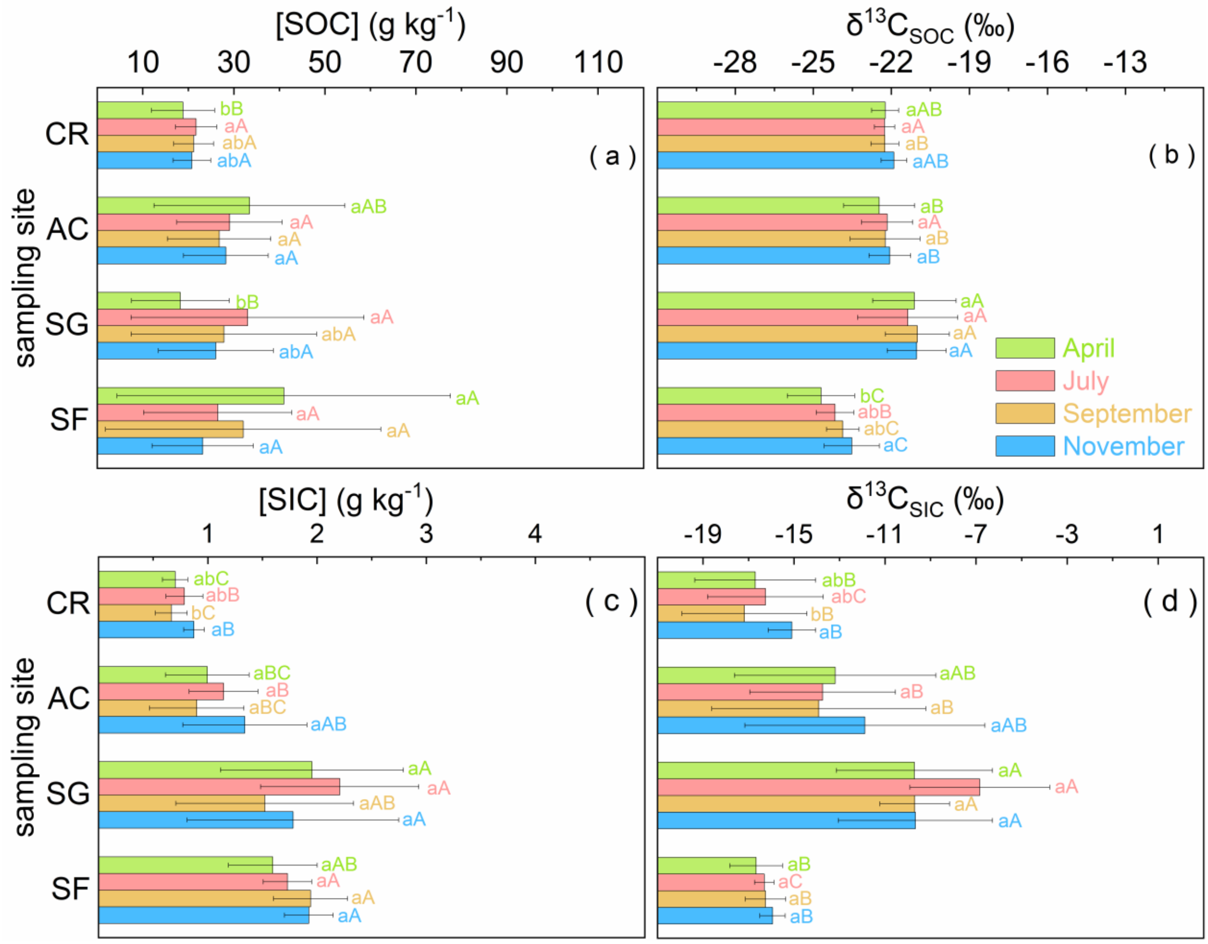

Figure 3: Seasonal variations of [SOC] (a), δ13CSOC (b), [SIC] (c), and δ13CSIC (d) in four land-use soil profiles. Different lowercase letters and uppercase letters denote significant differences among diverse season in the same land use and among diverse land uses in the same season, respectively (one-way ANOVA, Duncan post-hoc test, $P < 0.05$). CR, AC, SG and SF refer to cropland, abandoned cropland, shrub-grassland and secondary forest, respectively.

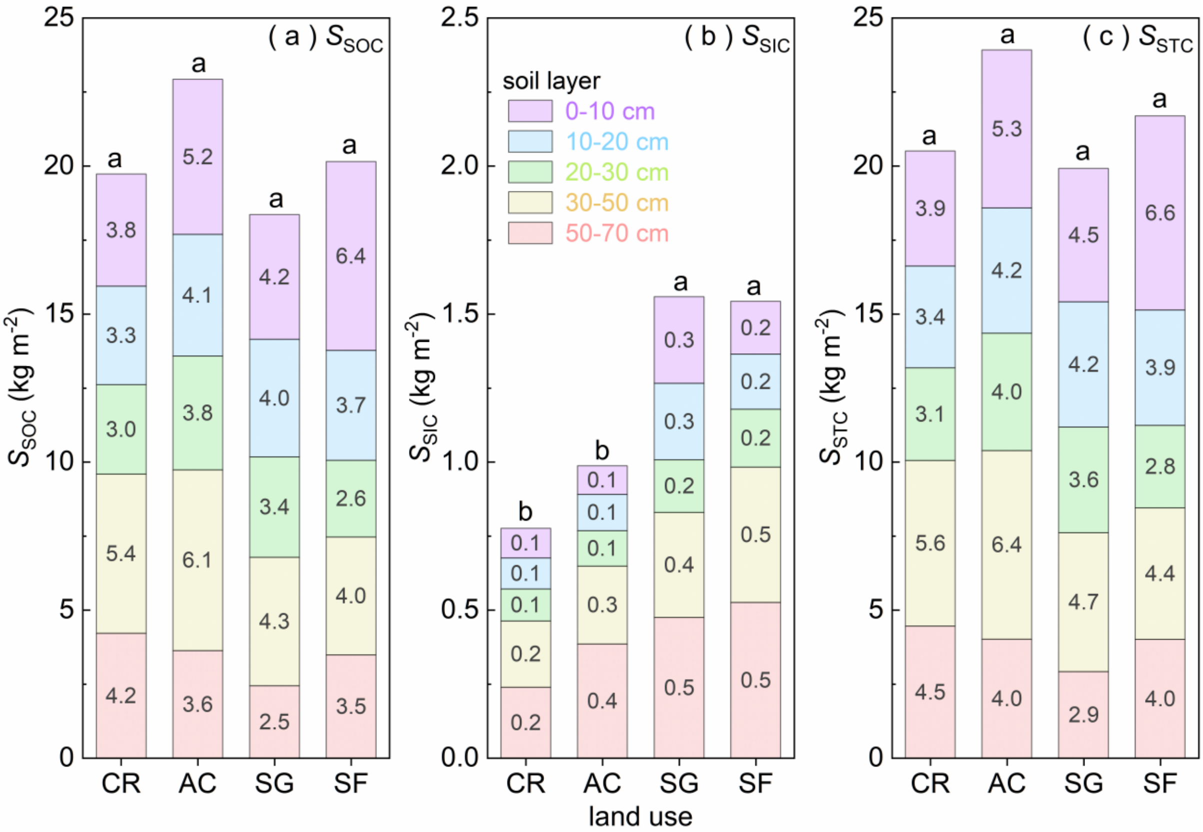

Figure 4: Vertical distributions of SOC, SIC and STC stocks (SSOC, SSIC and SSTC) in four land uses. CR, AC, SG and SF refer to cropland, abandoned cropland, shrub-grassland and secondary forest, respectively. Different lowercase letters denote significant differences of C stock (0–70 cm layer) among diverse land uses (one-way ANOVA, Duncan post-hoc test, $P < 0.05$).

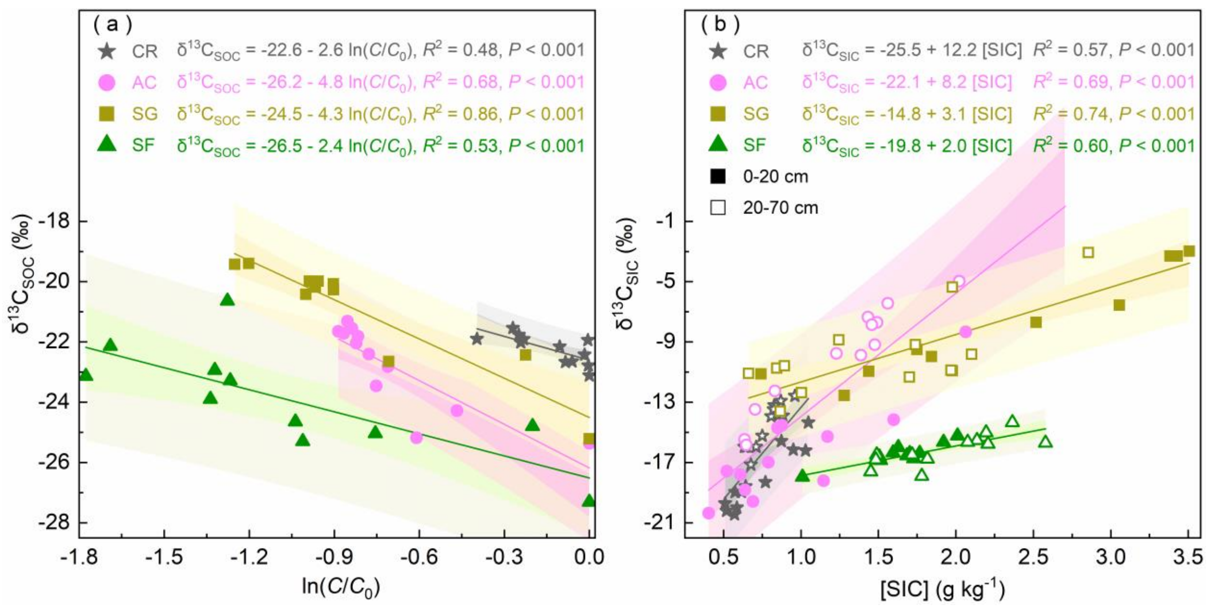

Figure 5: (a) Correlation between ln(C/C0) and δ13CSOC values in 0–20 cm soil layer of diverse land uses. C and C0 refer to [SOC] corresponding to δ13CSOC and the highest [SOC] in the surface soil (0 cm) of individual land uses, respectively. (b) Relationship between [SIC] and δ13CSIC in diverse land uses. CR, AC, SG and SF refer to cropland, abandoned cropland, shrub-grassland and secondary forest, respectively.

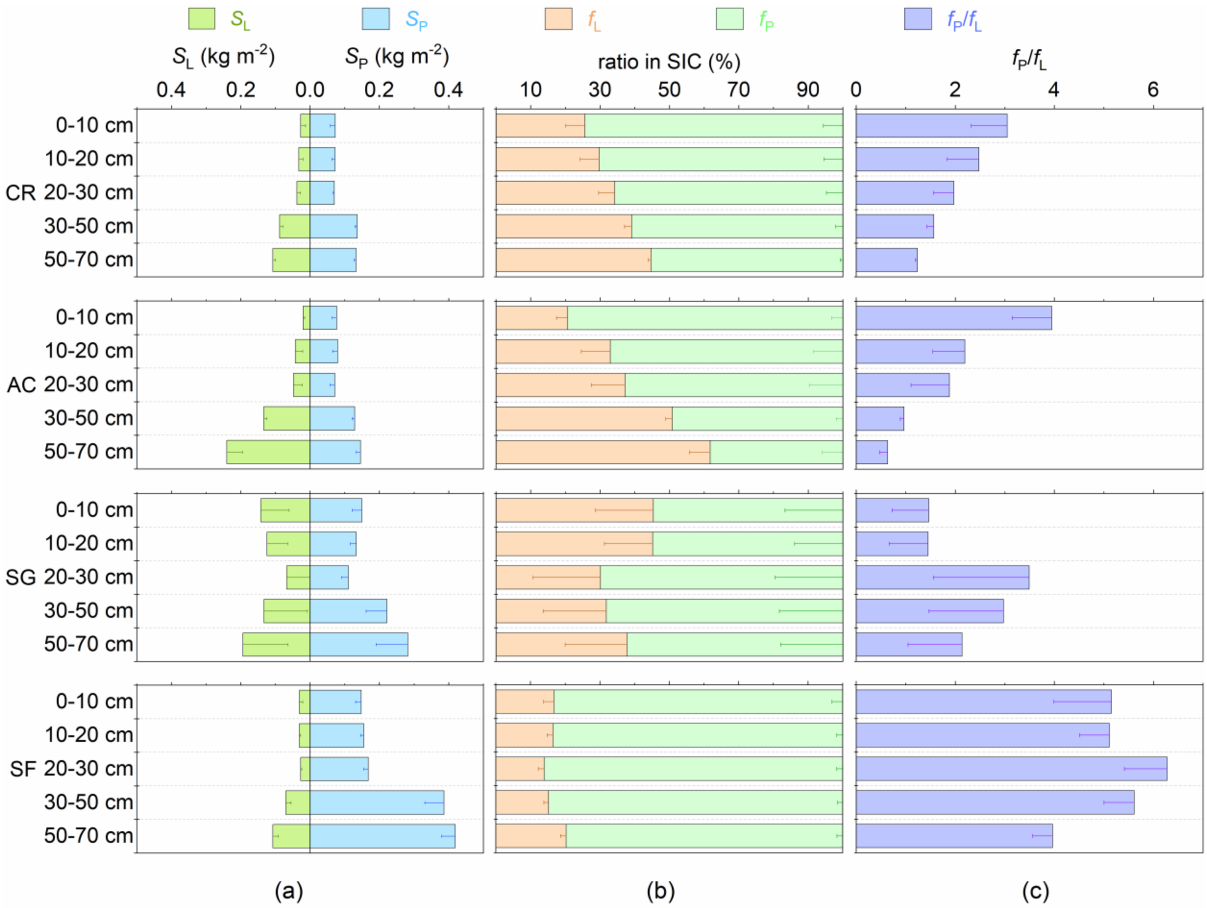

Figure 6: Vertical variations of lithogenic and pedogenic stocks (SL and SP) and their proportions in SIC (fL and fP) in four land uses. CR, AC, SG and SF refer to cropland, abandoned cropland, shrub-grassland and secondary forest, respectively.